DIGITAL IMAGE CORRELATION TO ANALYZE NONLINEAR ELASTIC BEHAVIOR OF MATERIALS

Nirusha Phillips[a], Ghulam Mubashar Hassan[b], Arcady Dyskin[a], Cara MacNish[b], Elena Pasternak[a],

[a] School of Civil, Environmental and Mining Engineering, The University of Western Australia, Australia
[b] School of Computer Science & Software Engineering, The University of Western Australia, Australia
{21457355@student, ghulam.hassan@, arcady.dyskin@, cara.macnish@, elena.pasternak@}uwa.edu.au

Abstract

Photogrammetry and image processing have been used extensively to examine surface deformations. Digital Image Correlation (DIC) detects the two-dimensional subpixel displacements between two images in order to analyze deformations in geomechanical structures. In this study, the case of large deformations involving nonlinear elastic behavior of the material has been examined with the use of a physical model of Ethylene Vinyl Acetate (EVA) foam subject to axial strain up to 15%. The associated strain and displacement fields are reconstructed using DIC and compared with the Finite Element Method. DIC is used to analyze the critical hysteresis effect of the material which occurs during loading and unloading process. The results show that DIC is a reliable technique to analyze the nonlinear elastic behavior of materials.

1. Introduction

Digital Image Correlation (DIC) is an image processing technique which can be used to determine the behavior of elements of a material under unspecified loading conditions. DIC, first used in the 1980s, has been used to obtain reliable stress and strain data of surfaces without physical contact with the surface [1].

A photograph of the undeformed specimen, the *reference image* is compared with an image of the deformed object, the *deformed image*. Sections of the image, subsets, are compared to determine the most likely displacement of each pixel and the displacement and strain fields developed in the object are reconstructed.

Materials such as rubbers exhibit unique properties which can be used to our advantage. The relationship between the material composition and behavior can be complex when the material exhibits non-linear behavior upon loading.

In this study, DIC is proposed as a technique to analyze the strains experienced by rubber. An experiment is devised by means of a sheet of Ethylene Vinyl Acetate (EVA) foam under axial loading conditions. Images of the material under prescribed displacements have been captured, and DIC has been used to reconstruct the strain and displacement fields. The accuracy and limitations of applying DIC to obtain this data has been investigated and compared with Finite Element Methods. One the other hand, the comparison also provided the model which is representing the material's characteristics in the better manner. The expected nonlinear behavior of the material while loading and unloading is analyzed and a hysteretic response has been captured.

2. Digital Image Correlation

DIC requires each point of the specimen's surface be uniquely identifiable [21, 24]. Therefore, the pattern on the surface of the specimen needs to have varying intensity in the area under consideration. Normally, a random speckle pattern is painted on the surface of the specimen [2, 16]. The scope of this study is to analyze planar deformation which is horizontal (x-direction) and vertical (y-direction) displacements of each point of the specimen.

Each pixel in the area of interest in the reference image is tracked in the deformed image, creating a series of data points which are mapped to create the displacement fields [3, 15, 18]. The distance of each point from the point of focus is described by the first order Taylor's expansion.

$$x^* = x + u + \frac{\partial u}{\partial x}\Delta x + \frac{\partial u}{\partial y}\Delta y \qquad (1)$$

$$y^* = y + v + \frac{\partial v}{\partial y}\Delta y + \frac{\partial v}{\partial x}\Delta x \qquad (2)$$

where *(x,y)* is the point of interest in the reference image and *(x*,y*)* denote the new position of the point *(x,y)* in the deformed image. *u* and *v* denote displacements of point *(x,y)* in horizontal and vertical directions respectively. The linear approximation in equations (1) and (2) are valid for small subset size. The correlation coefficient, S is calculated as [4, 22]

$$S\left(x, y, u, v, \frac{\partial u}{\partial x}, \frac{\partial u}{\partial y}, \frac{\partial v}{\partial y}, \frac{\partial v}{\partial x}\right) = 1 - \frac{\sum[F(x,y) * G(x^*, y^*)]}{[\sum F(x,y)^2 * \sum G(x^*, y^*)^2]^2} \qquad (3)$$

where *F* and *G* represents the grey intensity level at each point in the subset of the reference and deformed images respectively. The equation is minimized using the Newton Raphson method [4].

Traditionally DIC is applied to cases of small strain, but recently its use has extended to examine larger deformation [5, 25]. The image size and subset must be carefully chosen in relation to the expected deformation, image and speckle pattern [6, 17].

3. Hyperelastic material models

The energy (*E*) relationship for linearly elastic materials is described by the area under the stress-strain curve (*W*) as shown in Figure 1. Deformations in the linearly elastic range are likely to be reversible following the same stress path on loading and unloading.

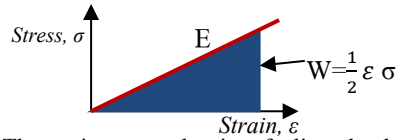

Figure 1: The strain energy density of a linearly elastic material

The stress-strain relationships for elastomers or hyperelastic materials are likely to have a non-linear relationship as this is outside of the linearly elastic range. For most solid rubbers, the behavior is reversible as demonstrated in Figure 2. Strains experienced by these materials can be large when relatively low stresses are applied. For example, the elastic modulus of steel is 200 GPa whereas the elastic modulus of natural rubbers experiencing small strains in the linear

region can be as low as 0.01GPa. Roylance demonstrated that when the material is stretched beyond the linearly elastic range, a rearrangement of its internal microscopic structure takes place [7]. The behavior has been described by a number of material models, all derived from the strain energy function, which are a function of the work done or energy dissipated as the material undergoes a physical change. The phenomenon is described by Figure 2. The shaded area illustrates the energy dissipated between loading and unloading the material. *Abb'cc'd* is the first time loading path while *b'Ba* and *c'Ca* are the unloading paths from point *b'* and *c'*.

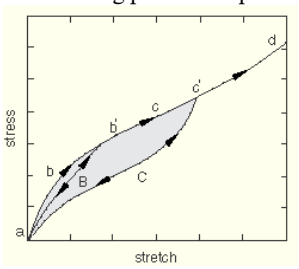

Figure 2: Diagram displaying nonlinear behavior & hysteresis [8].

The Ogden, Neo-Hookean and Mooney-Rivlin models used in this study are described as [9]

Ogden Strain Energy:

$$\bar{U} = \sum_{i=1}^{N} \frac{2\mu_1}{\alpha_1^2}\left(\overline{\lambda_1^{\alpha}} + \overline{\lambda_2^{\alpha}} + \overline{\lambda_3^{\alpha}} - 3\right) + \frac{K_1}{2}(J-1)^2 \qquad (4)$$

Neo-Hookean Strain Energy:

$$\bar{U} = \frac{\mu_1}{2}(\bar{I}_1 - 3) + \frac{K_1}{2}(J-1)^2 \qquad (5)$$

where λ_i symbolizes principal stretch directions, $\overline{\lambda_i} = \lambda_i / J^{\frac{1}{3}}$ and J[2] is the determinant of the left Cauchy-Green tensor. μ_1, K_1 and α_1 represent shear modulus, bulk modulus and material constant while $\bar{I}_1 = {J^{-2/3}}/{I}$ and I is the first invariant of the right Cauchy-Green deformation.

The Generalized Mooney-Rivlin model:

$$\bar{U} = \frac{\mu_1}{2}(\bar{I}_1 - 3) + \frac{\mu_2}{2}(\bar{I}_2 - 3)\ \frac{K_1}{2}(J-1)^2 \qquad (6)$$

where μ_1, μ_2 and K_1 are material constants. The variables I1 and I2 are the first and second invariant of the left Cauchy-Greem deformation respectively and $\bar{I}_1 = {J^{-2/3}}/{I_1}$ and $\bar{I}_2 = {J^{-4/3}}/{I_2}$.

4. Finite Element Method

Finite Element Method (FEM) is a well-known technique to analyze the non-uniform deformation model with high accuracy. It discretizes a solid into elements whose individual deformation behavior is characterized by the material model chosen, and affected by the boundary conditions and loading parameters. The deformation of each individual element is related to adjacent elements via nodes, contributing to the overall deformation of the solid.

5. Experimental Setup

It was necessary to apply a prescribed axial displacement to a material (a known axial strain) in order to test whether DIC can be applied to cases of large strains, such as up to 15% strain. Hence, apparatus was designed as shown in Figure 4 to apply a measured tension to one edge of a material while keeping the other end fixed.

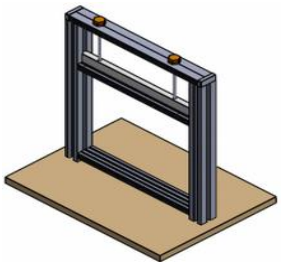
Figure 4: The device used to apply tension to the EVA specimen.

The apparatus was developed by the University of Western Australia's Workshop. The tension rig is designed in such a way that one turn of each upper bolt results in a 1 mm displacement of the top edge of the material.

Ethylene Vinyl Acetate foam (EVA) is the elastic material selected for this experiment. The material has a matte texture, so noise caused by reflection of light during the image capturing process is minimized. Several specimens of the EVA foam of dimensions 200 x 250 mm (length x height) were used. Speckle patterns of varying sizes were applied described as three sizes: large speckles of diameter 5-7 mm, medium speckles of diameter 4-6 mm and small speckles of diameter 3-4 mm. A Canon EOS 5D Mark II camera was used to capture the images. The specimen was firmly secured to the bottom edge and the moveable top edge which is controlled by tension mechanism.

After calibrations, images were taken as the material was stretched in 5 mm increments. The increment is chosen to maximize efficiency with a suitable subset size for implementing DIC. The images were cropped to the area of interest to be used in DIC.

The six parameters are optimized as mentioned in equ. (5), which are u and v representing displacements in horizontal and vertical directions respectively, $\frac{\partial u}{\partial x}$ and $\frac{\partial v}{\partial y}$ representing normal strains and $\frac{\partial u}{\partial y}$ and $\frac{\partial v}{\partial x}$ representing the components of shear strain.

6. Finite Element Simulations

Finite Element Methods software, ANSYS has been harnessed to discretize the material into elements. Boundary conditions and displacements are applied to determine the deformation characteristics of each element. The choice of element size has been driven by the output of DIC, such that each element has displacement and strain parameters described by the DIC output and by the Finite Element Analysis output.

Firstly, the material is divided into a 350 x 350 grids using a Plane182 element model with 3 mm thickness. The boundary conditions and loading conditions are:

1) Fixed in three degrees of freedom on the base edge,
2) Fixed in the horizontal direction on the top edge, and
3) Prescribed displacement on the top edge for varying strain

Three different material models were applied. One of the Mooney-Rivlin models used a 2-parameter form, as guided by Altidis & Warner [10] while the other Mooney-Rivlin model was guided by Cheung & Zhang [11]. The Ogden material constants were guided by MSC Software Corporation [12]. The input for a Neo-Hookean model [13] is the shear modulus of the material calculated experimentally. The material inputs are presented in Table 1.

Table 1: Material parameters used in ANSYS simulations

Model	Input Parameters
Mooney-Rivlin [10]	C10 = 0.162 C01 = 0.041
Mooney-Rivlin [11]	C10 = 0.08556 C01 = -0.05841
Ogden [12]	$\mu_1 = 0.63$MPa $\mu_2 = 0.0012$MPa $\mu_3 = 0.01$MPa $\alpha_1 = 1.3$ $\alpha_2 = 5.0$ $\alpha_3 = 2.0$
Neo-Hookean [13]	Ogden Shear Modulus μ = 220kPa

7. Results and Discussion

The displacement and strains field are reconstructed using DIC and the results are compared with the results of the model simulated using the Finite Element Method.

7.1 Recovery of Displacement field

The horizontal and vertical displacement fields of the specimen at each point of extension are reconstructed. Figure 5 and 6 presents the displacement fields reconstructed by DIC when the material is extended to 30 mm displacement at the top edge. The total extension applied to the specimen was 30 mm; and the maximum vertical displacement reconstructed by DIC was 25 mm. The difference of 5 mm is due to the fact that original images were cropped to the size of the initial reference image.

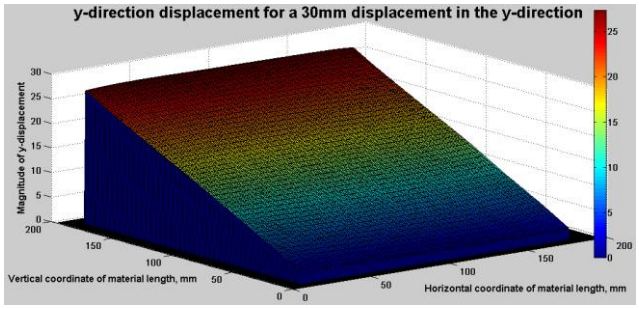

Figure 5: The reconstructed vertical displacement field.

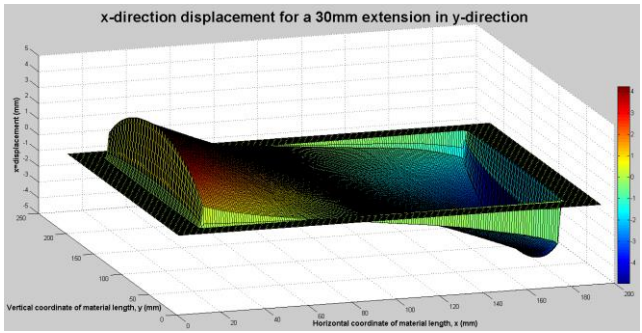

Figure 6: The reconstructed horizontal displacement field

7.2 Recovery of Strain field

The strain fields are reconstructed using the result of DIC. The reconstructed normal strain in the vertical direction is presented in Figure 7. The extension of 30 mm in the specimen of length 200 mm introduces 15% strain which is considered as large strain. It is observed that vertical normal strain is constant over the surface.

The reconstructed horizontal normal strain field is presented in Figure 8. It shows that strain varies over the surface of the specimen and is zero at point of clamping in the apparatus as the material is affixed to the apparatus at these regions. The strain is high at the center of the specimen along the vertical direction.

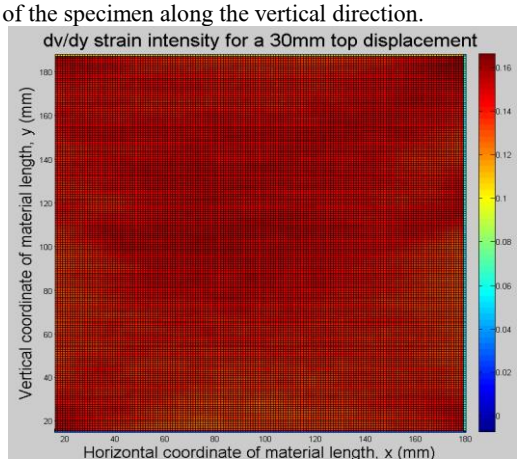

Figure 7: The reconstructed vertical normal strain field.

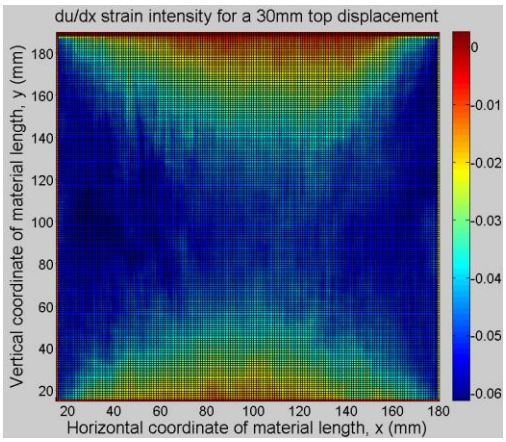

Figure 8: The reconstructed horizontal normal strain field.

7.3 Comparison with simulated Finite Element Method results

Finite Element simulations have been executed using four models; Ogden, Mooney Rivlin 2-parameter model with two different sets of parameters, and the Neo-Hookean model with details in Table 1.

The difference of results of simulated models by FEM and the results of DIC are plotted in Figure 9 and 10 for horizontal and vertical normal strains respectively. It is found that DIC works well for the vertical direction normal strain where the relative error is in the range of 0.6% to 2.5% as presented in Figure 9. On the other hand, the horizontal direction normal strain yields a high relative error as shown in Figure 10 for all models. This discrepancy exists because the absolute magnitude of normal strain introduced in the specimen is of the order of 14% to 16% in the vertical direction as compared to 0% to 6% in the horizontal direction. The results highlight the limitation of DIC to measure very small strain as discussed in [20, 23]. The results also show that Ogden model is the most fitting model for EVA. In summary, DIC is able to accurately measure the displacements and strains introduced by strains up to 15%.

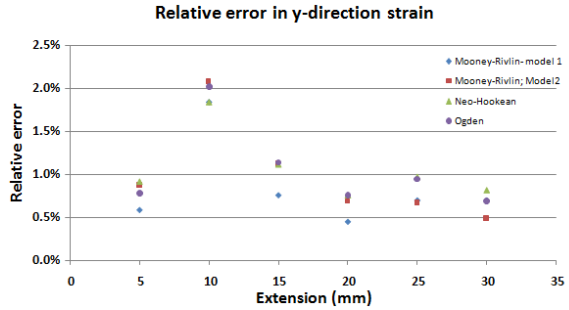

Figure 9: Relative error between ANSYS strain output and DIC output in the vertical direction.

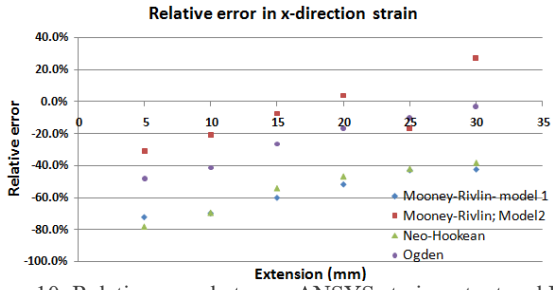

Figure 10: Relative error between ANSYS strain output and DIC output in the horizontal direction

7.4 Hysteretic Response

A very interesting observation in analysis of the results was the difference in strains recovered by DIC before and after extending the specimen to maximum extension of 30 mm. This observation is known as hysteresis due to the change in the microscopic structure of the material upon loading in the nonlinear range.

Upon discovering the property of hysteresis, a simple estimate of the stress-strain relationship of the material upon loading and unloading has been carried out in the laboratory. A fishhook scale was used to measure the mass and therefore the force applied by the apparatus in order to maintain the required extension.

This procedure is expected to be limited in accuracy; however a reasonable value of initial elastic modulus of 0.62 MPa has been determined for the specimen, which is close to the value of 0.65 MPa as mentioned by Song and Shisheng [14, 19]. DIC also validated the same in our experiments. Using the same procedure, the hysteretic effect of loading and unloading the EVA foam is obtained and presented in Figure 11.

The behavior of a foam elastomer under cyclic loading conditions is complex and a number of idealizations have been made to predict the behavior. The idealizations result in two components of the material behavior [8]

1) the response of a material element under monotonic strain, and
2) the material response associated with damage due to the loading mechanism.

Upon removing the material from the apparatus, the vertical direction normal strain measured was 3%. Figure 12 shows the graph that demonstrates that the average vertical direction normal strain that the material experience is highest at a final displacement of 5 mm after unloading the specimen.

The results show that DIC successfully identifies the hysteretic effects upon unloading of the specimen. It is expected DIC can also be employed to determine the behavior of the material upon re-loading which is expected to follow a different stress path due to the cyclic loading of the specimen. This can be employed in future studies to study cyclic loading idealizations.

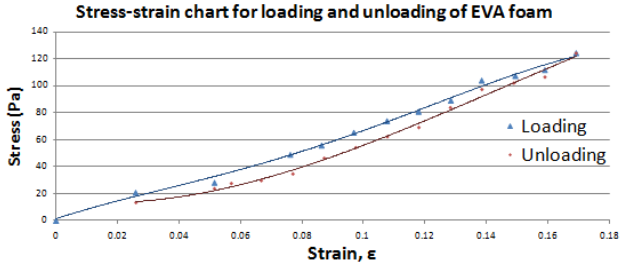

Figure 11: The estimate of a stress-strain diagram for the loading and unloading of the EVA foam specimen.

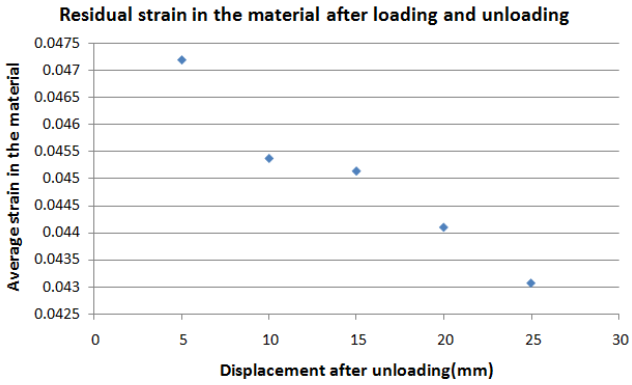

Figure 12: Average vertical direction strains measured by DIC during unloading of the specimen after loading to maximum

8. Conclusion

In this study, the performance of DIC is examined to measure large deformations and analyze the properties of the material. A physical experimental apparatus is designed and used to ensure that a hyperelastic behaving material is loaded under extension with successive images taken at each step. These images are processed using DIC and series of displacement and strain fields are reconstructed.

The displacement and strain fields reconstructed by DIC are compared with different models simulated in Finite Element simulations. The relative error in the vertical direction normal strain for all selected models for Finite Elements simulation was found to be 0.5% to 2%. However the relative error in the horizontal direction normal strain was found to be high of the order of 10% to 80% due to small introduced strains. Despite experimental errors, the errors of DIC results compared with the Finite Element simulations models are found to be low. The results also mentioned that Ogden model is best among the tested models to represent the deformation characteristics of the EVA foam material.

Another important finding in this study is the capability of DIC to recognize the hysteresis effects of the material as the material is loaded and un-loaded. This is an important characteristic for the number of materials and is a complex, time-dependent mechanism and not easily determined by a material model. The focus of this study is to show the capability of DIC to study the behavior of hysteresis effects and evaluate which existing hysteresis model is closer to real world problem.

References

[1] M.A. Sutton, W.J. Wolters, W.H. Peters, W.F. Ranson, and S.R. McNeill, "Determination of displacements using an improved digital image correlation method", Image and vision computing , 1983, pp.133-139.

[2] G.M. Hassan, C. MacNish, A. Dyskin, and I. Shufrin, "Digital Image Correlation with Dynamic Subset Selection", International Journal of Optics & Lasers in Engineering, vol. 84, pp.1-9, 2016.

[3] V. Pickerd, "Optimisation and Validation of the ARAMIS Digital Image Correlation System for use in Large-scale High Strain-rate Events", VIC: Maritime Division (Defence Science and Technology Organization of Australia), 2013.

[4] H. Bruck, S. McNeill, M. Sutton, and Peters, W., "Digital Image Correlation Using Newton-Raphson Method of Partial Differential Correction", Experimental Mechanics, pp.261-267, 1989.

[5] Y. Zhou, B. Pan, and Y. Chen, "Large deformation measurement using digital image correlation: a fully automated approach", Applied optics, pp.7674-7683, 2012

[6] D. Lecompte, A. Smits, S. Bossuyt, H. Sol, J. Vantomme, D. Van Hemelrijck, and A.M. Haberaken, "Quality assessment of speckle patterns for digital image correlation", Optics and Lasers in Engineering , pp.1132-1145, 2006

[7] D. Roylance, "Mechanical Properties of Materials", MIT 2008.

[8] R. Ogden, and D. Roxburg, "A Pseudo-Elastic Model for the Mullins Effect in Filled Rubber", Proceedings of the Royal Society of London (Series A, vol. 455, pp.2861–2877). London: Royal Society of London, 1999.

[9] A.F. Bower, "Applied Mechanics of Solids", CRC Press 2012.

[10] P. Altidis, and B. Warner, "Midwest ANSYS Users Group: Analyzing Hyperelastic Materials", Wisconsin, America: Impact Engineering Solutions, 18 May 2005.

[11] J.T. Cheung, and M. Zhang, "Finite Element Modeling of the Human Foot and Footwear", ABAQUS Users' Conference, (pp.15), Hong Kong, 2006.

[12] MSC Software Corporation, "Nonlinear Finite Element Analysis of Elastomers", Texas: MSC Software, 2015.

[13] M. Jenkins, "Materials in Sports Equipment", Cambridge: CRC 2003.

[14] L. Song, and H. Shisheng, "Testing the compressive property of EVA foam at high strain rate", Society for Experimental Mechanics, China: Chinese Academy of sciences, 2003.

[15] P. Bing, X. Hui-min, X. Bo-qin, and D. Fu-long, "Performance of sub-pixel registration algorithms in digital image correlation", Measurement Science and Technology, pp.1615–1621, 2006.

[16] S. Bossuyt, "Optimized patterns for digital image correlation", Annual Conference on Experimental and Applied Mechanics, Springer Science, 2013.

[17] A. Hijazi, A. Friedl, and C.J. Kähler, "Influence of Camera's Optical Axis Non-perpendicularity on Measurement Accuracy of Two-dimensional Digital Image Correlation", Jordan Journal of Mechanical and Industrial Engineering , pp. 373-382, 2011.

[18] T.J. Keating, P.R. Wolf, and F.L. Scarpace, "An improved method of Digital Image Correlation", Photogrammetric Engineering and Remote Sensing , pp. 993-1002, 1975.

[19] R. Verdejo, and N.J. Mills, "Heel-shoe interactions and the durability of EVA foam running-shoe midsoles", Journal of Biomechanics , pp.1379-1386, 2004.

[20] N.V. Dinh, G.M. Hassan, A. Dyskin, and C. MacNish, "Digital image correlation for small strain measurement in deformable solids and geomechanical structures", 2015 IEEE International Conference on Image Processing (ICIP), pp.3324-3328, 2015.

[21] G.M. Hassan, C. MacNish, and A. Dyskin, "Extending Digital Image Correlation to Reconstruct Displacement and Strain Fields around Discontinuities in Geomechanical Structures under Deformation", 2015 IEEE Winter Conference on Applications of Computer Vision (WACV), pp.710-717, 2015.

[22] G.M. Hassan, A. Dyskin, C. MacNish, and N. Dinh, "A Comparative Study of Techniques of Distant Reconstruction of Displacement Fields by using DISTRESS Simulator", Optik – International Journal for Light and Electron Optics, vol. 127(23), pp.11288-11305, 2016.

[23] David Hang, Ghulam Mubashar Hassan, Cara MacNish, and Arcady Dyskin, "Characteristics of Color Digital Image Correlation for deformation measurement in geomechanical structures", 2016 International Conference on Digital Image Computing: Techniques and Applications (DICTA), 2016.

[24] Gang Li, Ghulam Mubashar Hassan, Cara MacNish, and Arcady Dyskin, "Study of natural patterns on Digital Image Correlation using simulation method", International Journal of Computer, Control, Quantum and Information Engineering, vol. 9(2), pp344-351, 2015.

[25] C. MacNish, G.M. Hassan, A. Dyskin, and E. Pasternak, "Towards affordable and robust remote photogrammetric sensing for early warning of fracturing and structural failure", 2015 IEEE Region 10 Humanitarian Technology Conference (R10-HTC), pp.1-6, 2015.